FR09, Dec.7-11, 2009, Kyoto

Development of Integrated Analytical Tools for Level-2 PSA of LMFBR

December 8, 2009

K. Haga, H. Endo, T. Nakajima, T. Ishizu
Nuclear Energy System Safety Division
Japan Nuclear Energy Safety Organization (JNES)

H. Iizuka
MHI Nuclear Engineering Company

Contents

1. Background and Objectives

- **JNES is engaged in the technical support for the regulatory activity for Monju, the Nuclear and Industrial Safety Agency (NISA).**
- **The major areas of the supportive work are**

  Inspection and Safety analysis .
- **To the safety analysis, JNES has been developing the own tools for several years.**
- **Our reset big activity is the effectiveness evaluation of the proposed accident management (AM) of Monju by using PSA.**
- **The developed tools for the PSA are not only computer codes but also the decision method for the balancing points of event trees.**
- **This presentation presents the outline of each tool.**

Process of severe accidents of LMFBR and JNES's Analysis tools

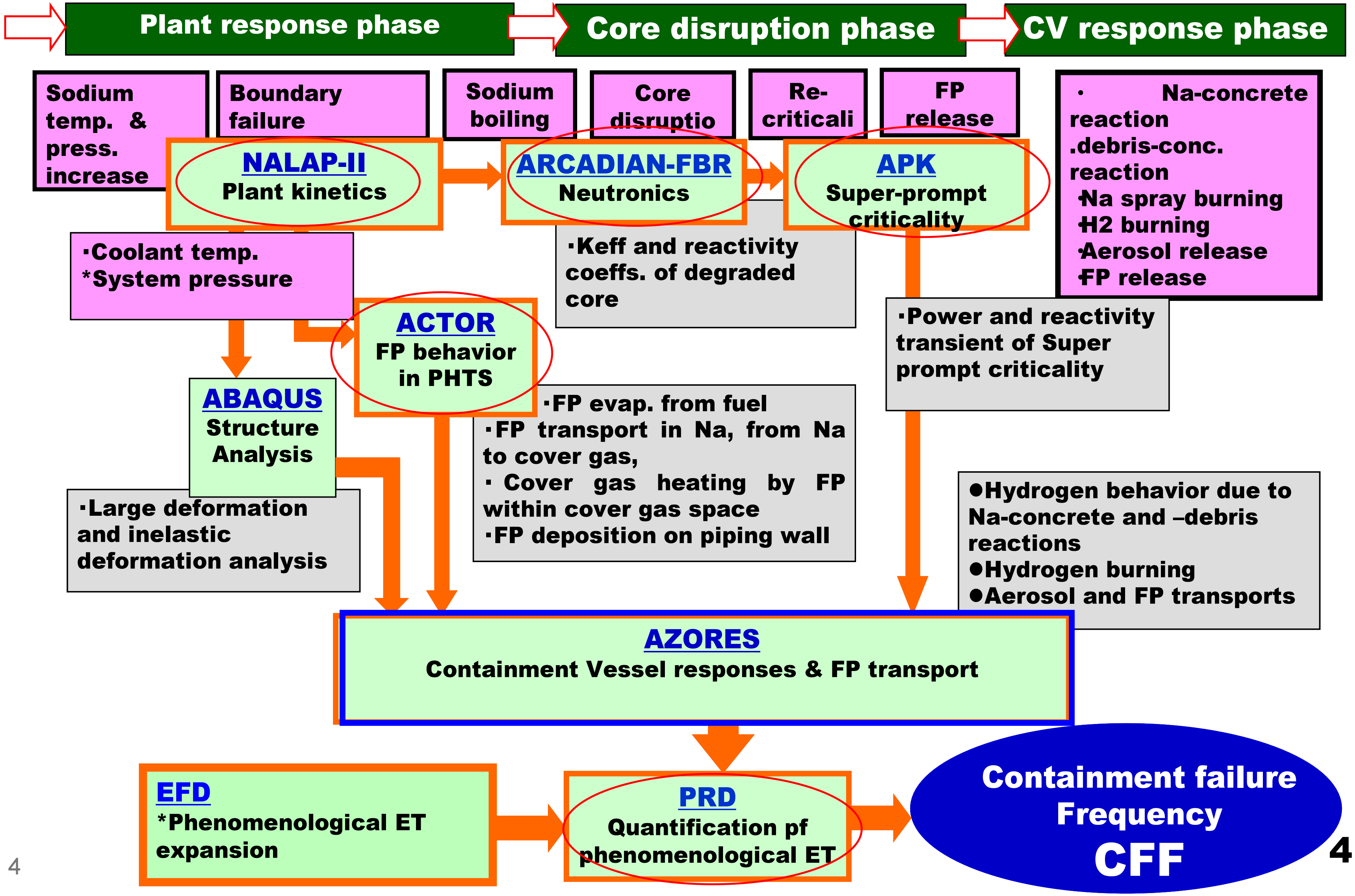

4

2. Computer codes

2.1 For the plant response phase（1）

NALAP-II code

Functions: Plant kinetics of the primary and secondary loops

Sales point: A function to evaluate the degree of high-temperature creep of the location by SCDF (Structural cumulative damage factor, D_c).

- $D_c = \Sigma(\Delta t_i / t_r)$, (1)

where,

Δt_i: computation time step (s),

t_r: creep failure time (s).

In eq. (1), t_r depend on the material, temperature and pressure. It is calculated by using the Larson-Miller Parameter.

It was considered that the location will fail when D_c=0.2～1.0

The thermo-hydraulic behavior analyzed by NALAP-II to PLOHS

-Reactor inlet and outlet temperatures, cover gas pressures, and SCDF of major locations-

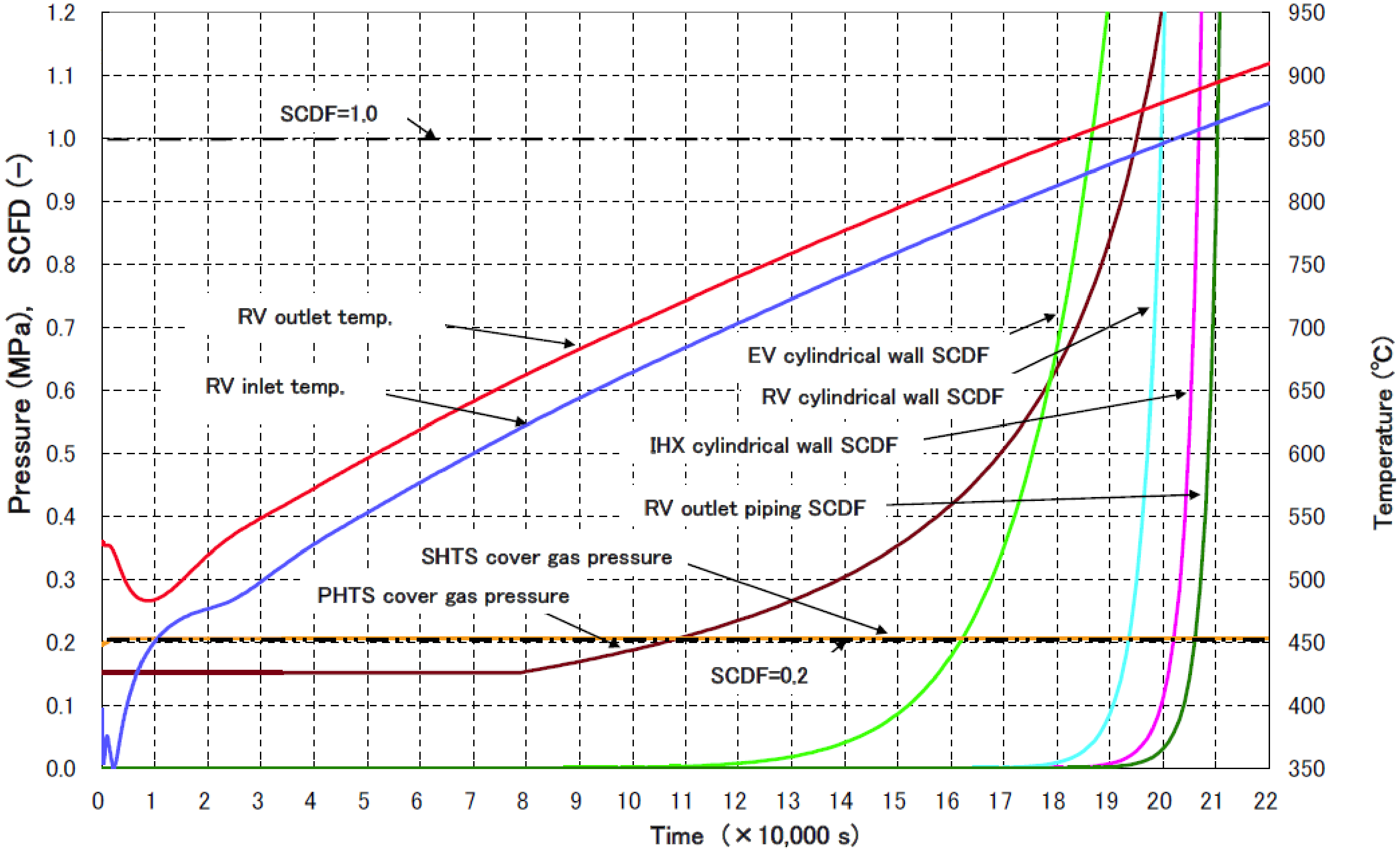

- **The RV outlet temperature exceeded 800℃ at 51hr.**
- **PHTS pressure began to increase at 22 hr due to the sodium volume expansion.**
- **The SCDF is evaporator cylindrical wall made of 2.25Cr-1Mo steel firstly exceeded the line of 0.2.**
- **Another locations exceeded the line of SCDF=0.2 after about 10 hr.**

2.1 For the plant response phase(2)

[ACTOR code]

Functions: FP behavior from fuel to cover gas or flowing sodium

Cover gas

Fuel → Bubble

Sodium → Primary loop

Sales point: Analysis of FP gas bubble behavior with other FP nuclides

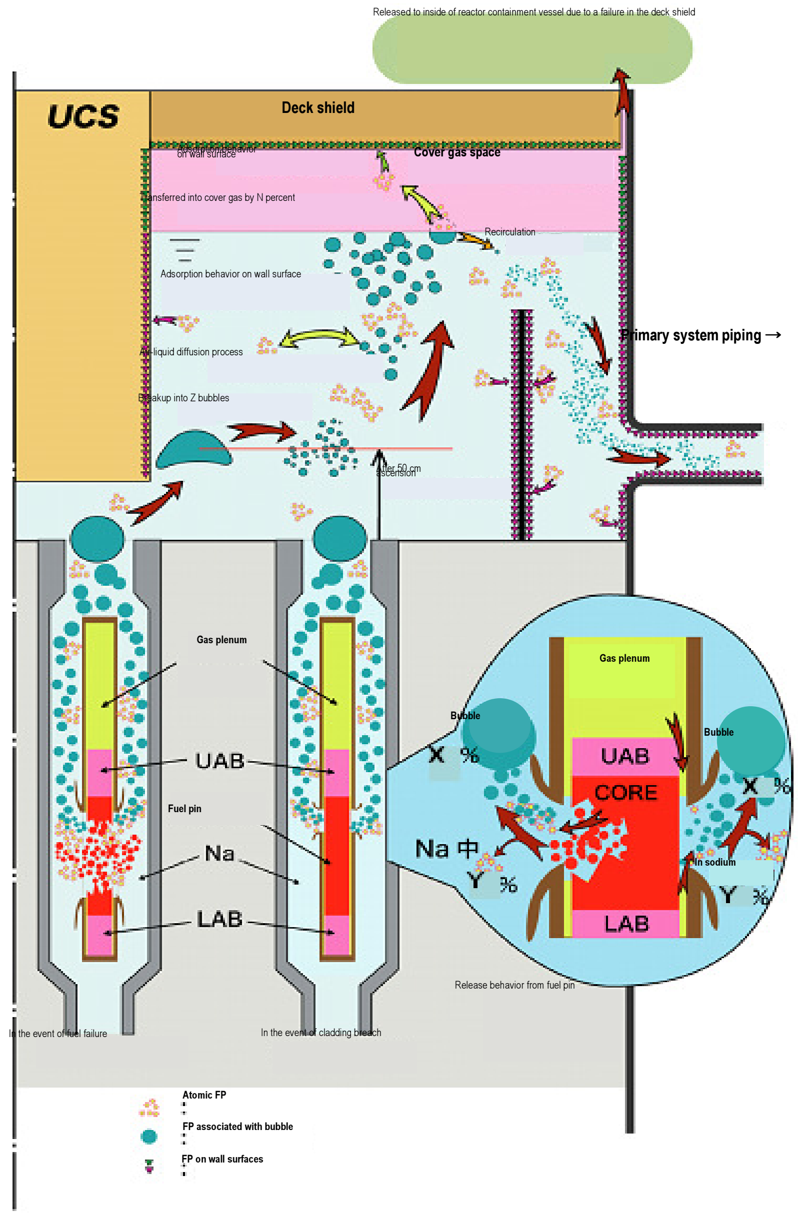

Calculations by ASFOR

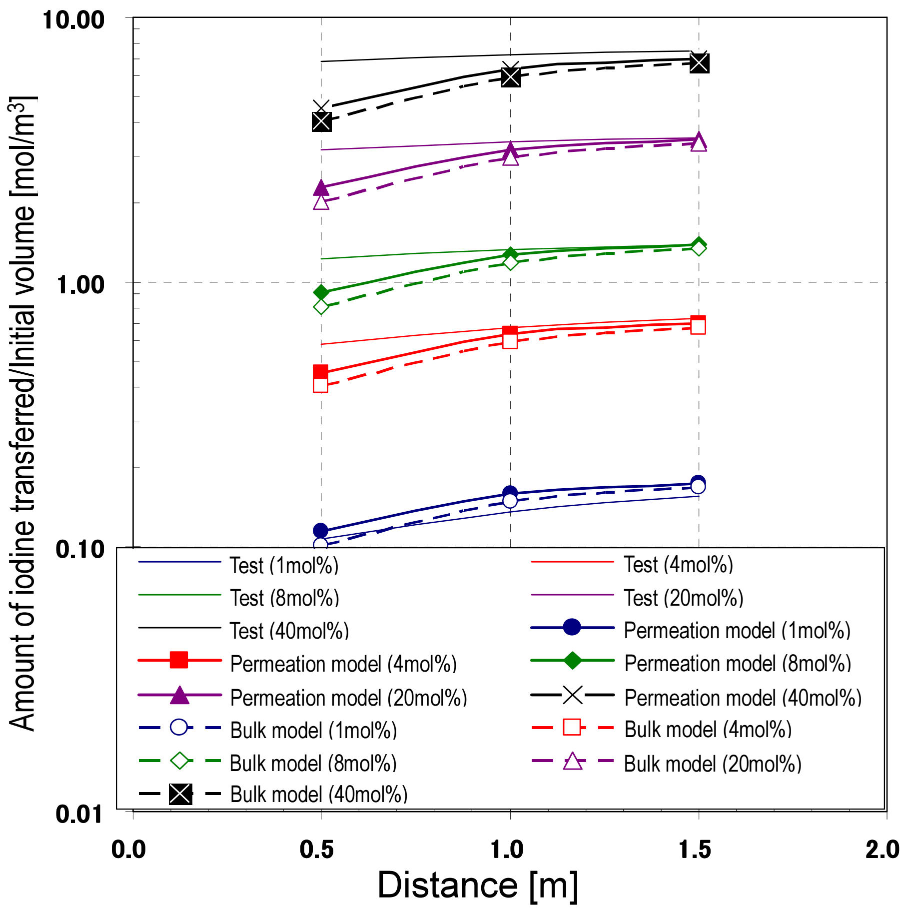

Amount of iodine transferred per bubble volume: Experiment & Calculation

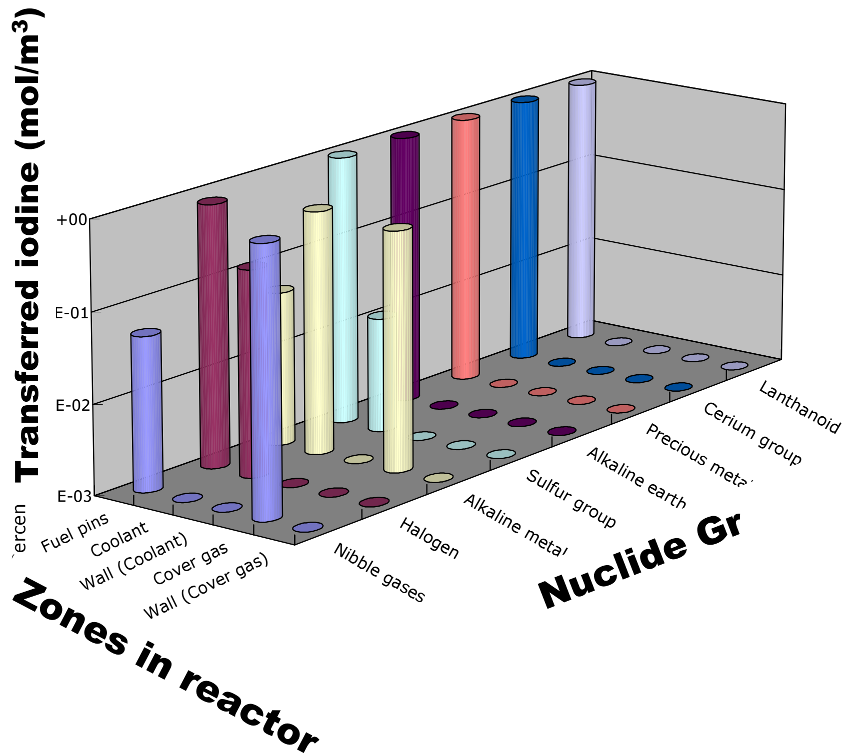

Distribution of FP nuclides in reactor 100s after cladding failure in PLOHS

2.2 For the core disruption phase (1)

ARCADIAN-FBR code

Functions: Neutronics for degraded core

Sales point: The combination of

(1)a deterministic calculation part

to provide the various reactivity coefficients and those spatial distributions

and

(2) a Monte Carlo calculation part

to provide reference results against the deterministic calculations and to evaluate approximation effects employed in the deterministic calculations

Constitution of ARCADIAN-FBR

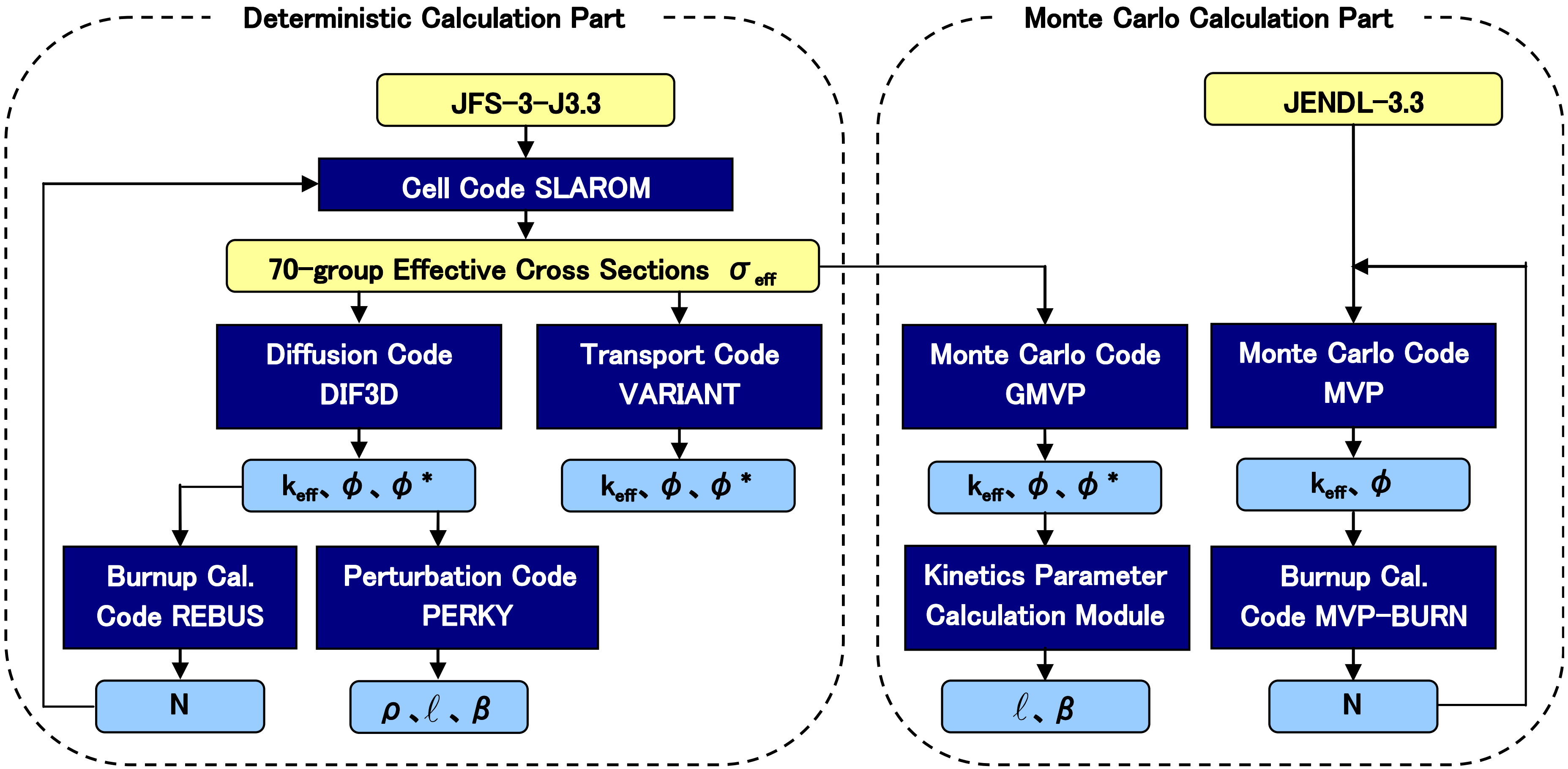

2.2 For the core disruption phase (2)

APK code

Functions: Reactivity evaluation by solving 6-group point reactor kinetics equations to debris beds of some temperature

Sales point: Simple using one point temperature

Validation: Comparison with SAS4A

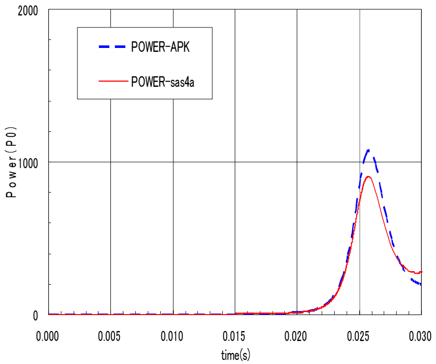

(a) Power history

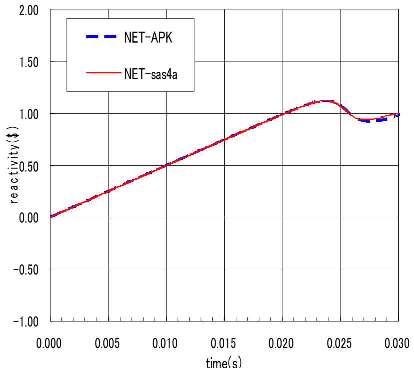

(b) Net reactivity

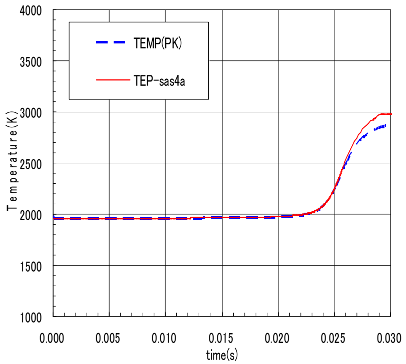

(c) Average fuel temp.

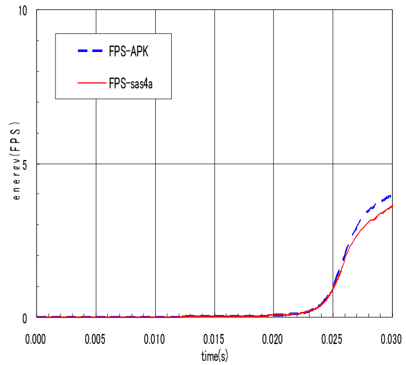

(d) Input energy

2.3 For the CV response phase

AZORES code

Functions: **To analyze various reactions caused by the sodium and core materials leaked through a failed coolant boundary.**

Sales point: **Radioactive materials behaviours to the environment are also solved with the thermo-chemical reactions.**

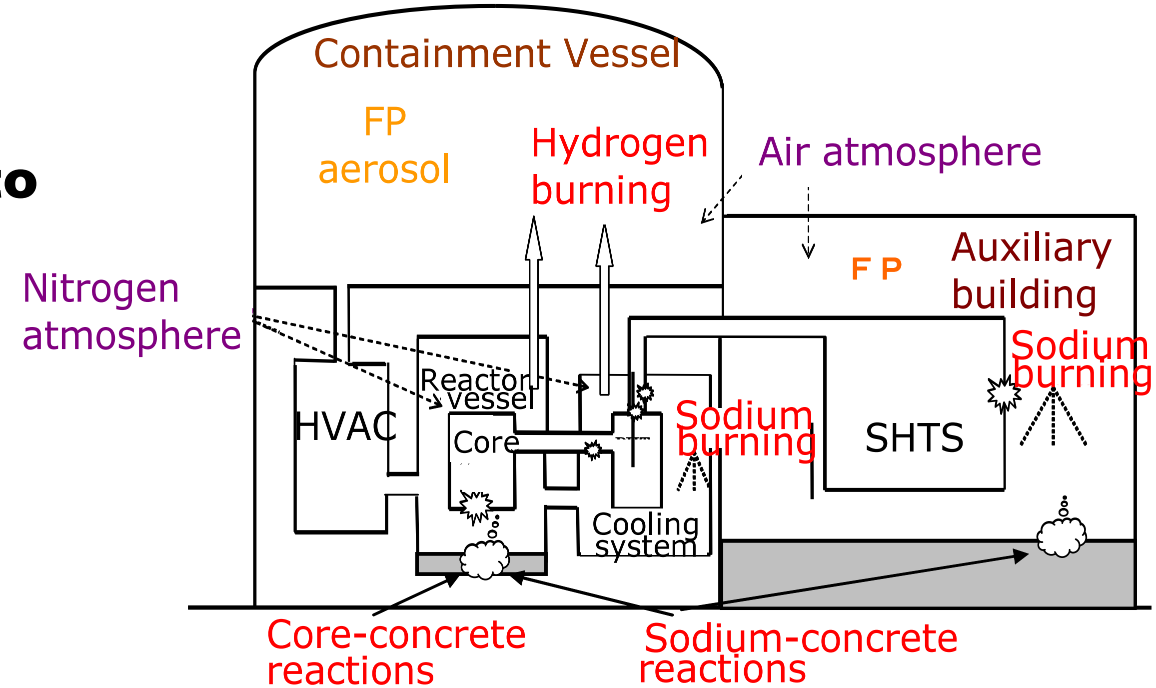

Example of CV response calculated by AZORES

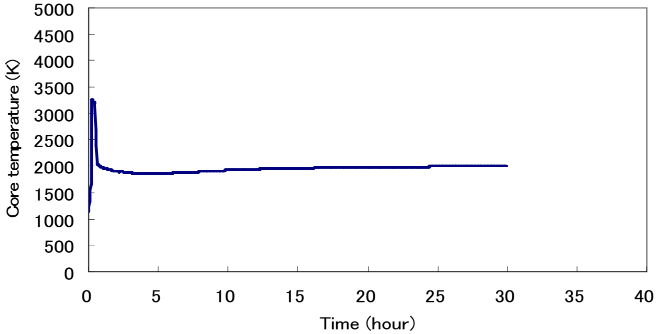

Fig. 7-22(1) Core Temperature (Case 15: PLOHS, Non-CVBP, PL-NSL-H-

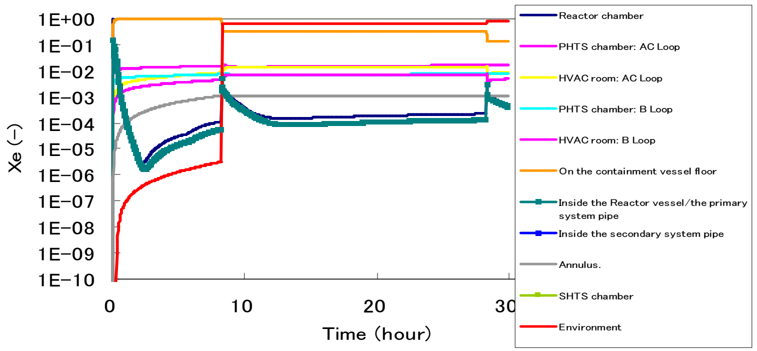

Fig. 7-23(1) Xe Gr Initial Inventory Ratio (Case 15: PLOHS, Non-CVBP PL-

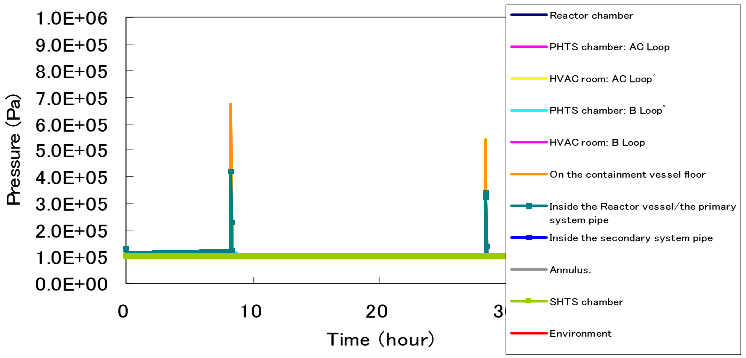

Fig. 7-22(2). Pressure (Case 15: PLOHS, Non-CVBP PL-NRL-H-

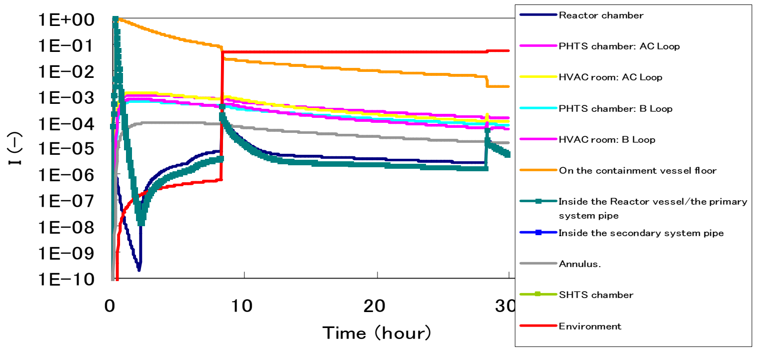

Fig. 7-23(2) I Gr Initial Inventory Ratio (Case 15, PLOHS, Non-CVBP PL-

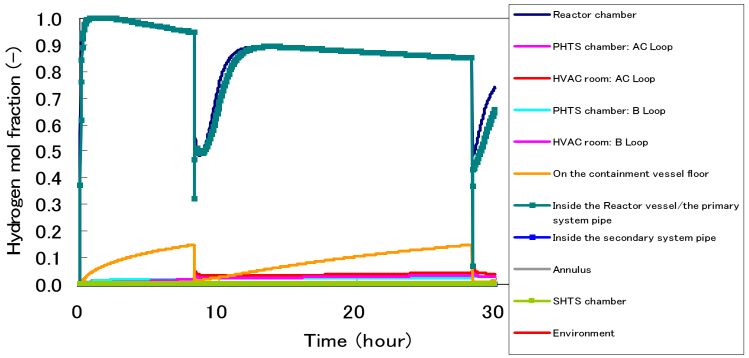

Fig. 7-22(3). Hydrogen Mol Fraction (Case 15: PLOHS, Non-CVBP, PL

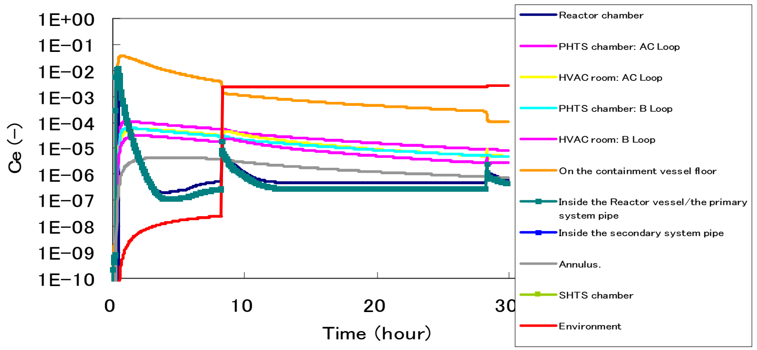

Fig. 7-23(3) Ce Gr Initial Inventory Ratio (Case 15:PLOHS, Non-CVBP PL-NRL-H-

3. Phenomenological Relation Diagram : PRD

Probability decision method for the blanching points in event trees (ET)

- **Objectives of PRD: To eliminate the subjective decision for the probability of blanching points in ETs.**
- **Procedure:**

(i) Constructs an event tree from the top event (an event considered at a branching point of an phenomenological event tree) to lower events.

(2) Function gate is settled to calculate by a certain function with lower events.

(3) To lower events the probabilities are to be give by any method as much as possible. The probability distributions are transferred to the upper events.

-PRD Appoach for the top event of acceleration -

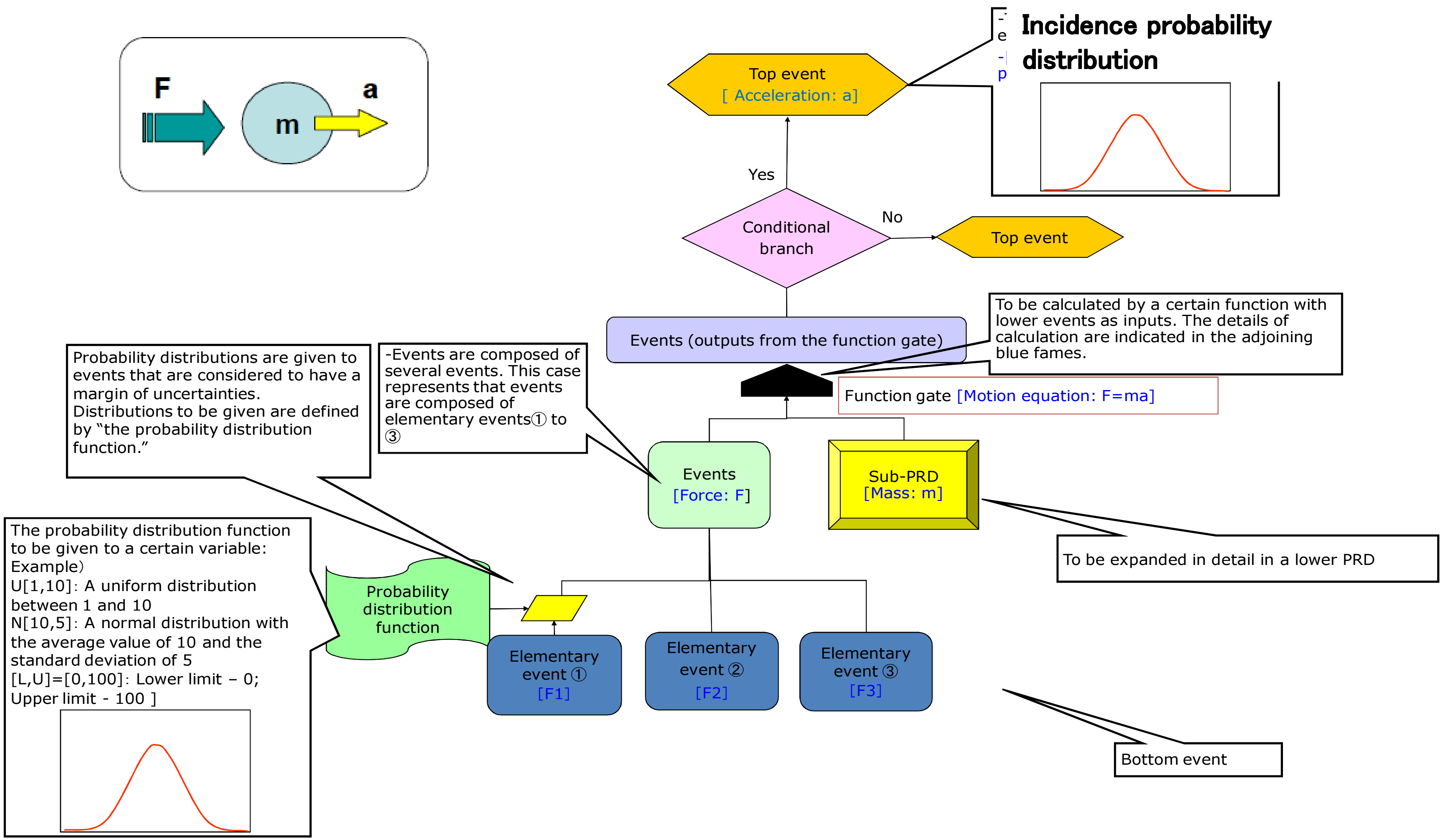

Evaluation procedures of ROAAM used LWR and PRD

ROAAM | PRD

(1) Selection of the dominant factors and development of diagram regarding the concerned phenomenon

- Select the dominant factors of the concerned phenomenon, break them down into low-order events, and relate them to each other.
- Develop the reciprocal relations among the lower-order events into a diagram

(2) Establishment of parameters of the dominant factors and introduction of probability distribution

- Parameters, which describe the concerned phenomenon, are classified into three categories including deterministic (D), probabilistic (P) and intangible variables (I).
- Establishment of the probability distribution regarding the P parameter of the developed lower-order events
- Establishment of the value based on engineering judgment regarding the I parameter

(3) Supplementary use of deterministic findings

- Establishment of the representative value of the lower-order events (D parameter) by using analysis based on the analytical codes, supported by a simple correlation equation
- Establishment of the representative value of the lower-order events (D parameter) supported by the empirical findings

(4) Evaluation of branching probability regarding the concerned phenomenon

- Evaluation of the branching probability of the concerned phenomenon, tracing the functional relation upwards using the Monte Carlo method and others

Both methods seem basically identical.

Summary

- **With the developed integrated analytical tools, one-through evaluation for severe accidents including FP release ratio became possible to LMFBR. The tools were used for the effective evaluation of AM for Monju.**
- **Now, further efforts are being made to make analyses more realistic for the Monju with an advance core and the Japanese demonstration LMFBR.**
- **These improvements are very helpful in constructing data-bases of the Emergency Response Support System (ERSS) for Monju by conducting more reliable analyses to the conceivable scenarios after initiating events.**

- **Many thanks for your audience.**

Characteristics of PLOHS

- **After the reactor shutdown, the plant temperature increases slowly but monotonously both in the primary cooling system (PHTS) and in the secondary cooling system (SHTS).**
- **Many plant locations will fail due to the high-temperature creep.**
- **Among several conceivable accident scenarios, the containment vessel by-bass (CVBP) would be most important event due to the high probability and the high potential of large scale FP release to the environment.**
- **We evaluated the frequency of PLOHS/CVBP in this study.**

FP leak passes in PLOHS/CVBP

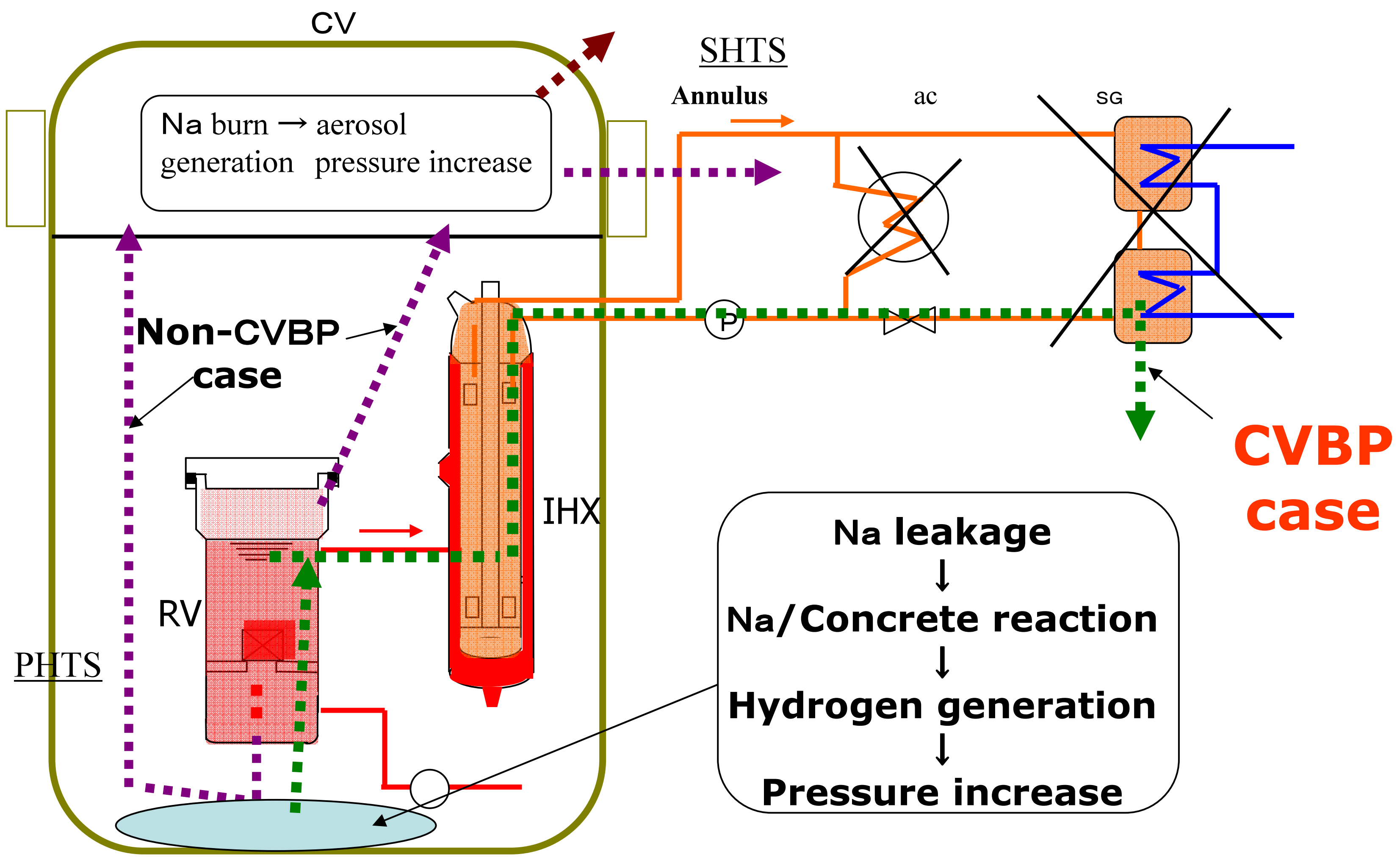

In the case of PLOHS/CVBP, some early failure in SHTS is postulated.

When some interface between PHTS and SHTS failed, FP from the molten fuel will run through PHTS and SHTS piping.

Boundaries of IHX that have a high potential of first failure in PHTS

Diameter: 700mm
Thickness: 1.5, 2.0 mm
Material: SUS3316

Cover gas bellows

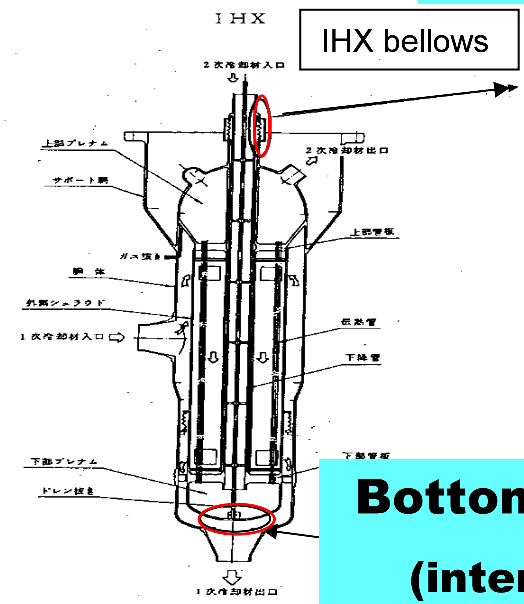

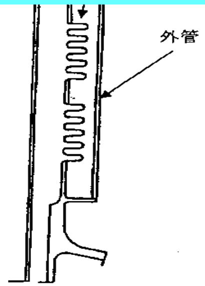

Bottom head

(interface between PHTS/SHTS)

Diameter: 2190mm
Thickness: 25mm
Material: SUS304

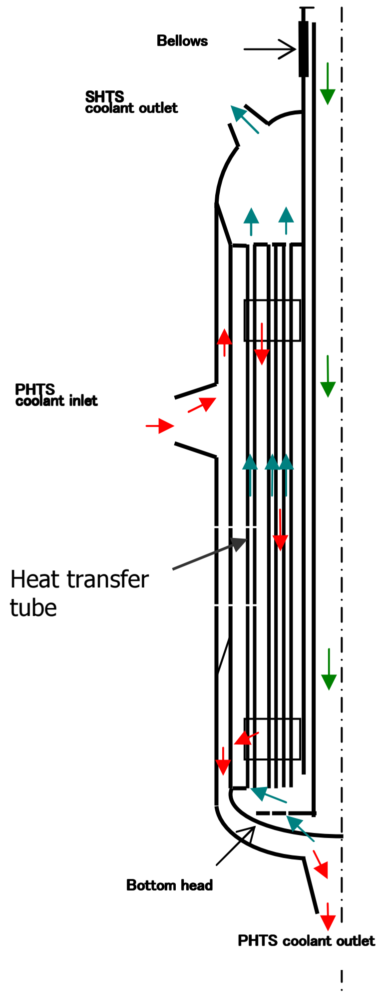

An vent tree of PLOHS

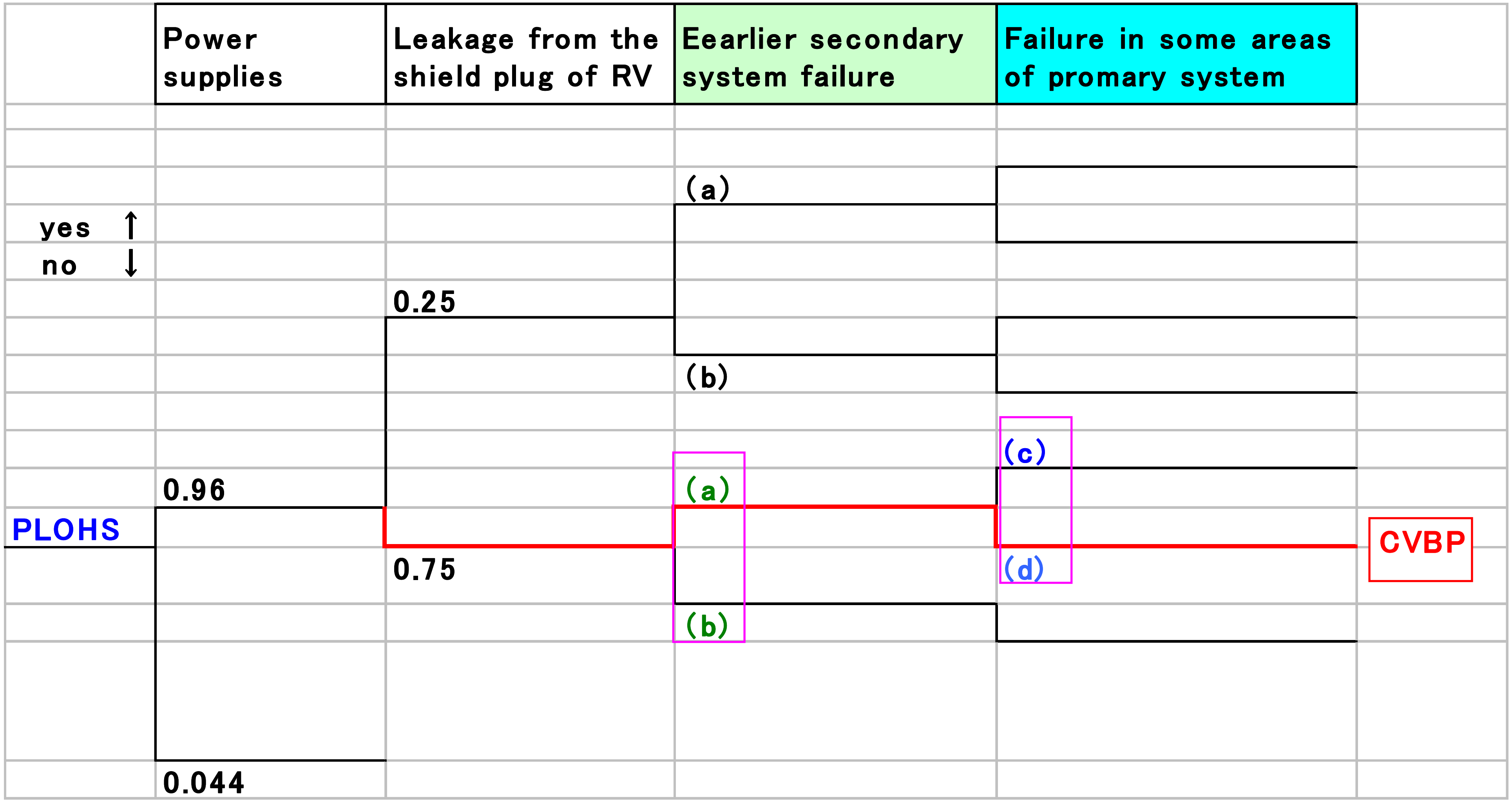

The probabilities of branching point (a), (b), (c),(d) are obtained through present analyses.

2. Analyses to obtain the probability of the branching points

Failure mechanism	Objects for analysis	Analysis code
High-temperature creep	Vessel, Piping	NALAP-II
Buckling Tensile (or breaking) stress	Bellows and bottom head of IHX	ABAQUS FINAS

Thermal-hydraulic Analysis (→ High-temperature creep)

Structual Analysis (→ Buckling, Tensile (or breaking) stress)

2.1 Thermal-hydraulic Analysis

FBR plant thermal-hydraulic analysis code NALAP-II

- **NALAP-II has been developed in JNES.**
- **For the present study a function was added to evaluate the degree of high-temperature creep of the location: SCDF (Structural cumulative damage factor, D_c).**

- $D_c = \Sigma(\Delta t_i / t_r)$, (1)

where,

Δt_i: **time step (s),**

t_r: **creep failure time (s).**

In eq. (1), t_r depend on the material and it is calculated by using the Larson-Miller Parameter.

It was considered that the location will fail when D_c=0.2～1.0.

Specifications of proto-type LMFBR plant and locations where high-temperature creep was evaluated

(a) Spec. of LMFBR

Thermal power	714 MW
Number of loops	3
Primary heat transfer system (PHTS)	
Temperature at reactor inlet/outlet	397/529 ℃
Flow rate	5100 t/h
Pressure at reactor inlet/outlet	0.8/0.1 MPa
Main circulatiion pump	One unit per loop
IHX	
Number of unit	3
Type	Vertical parallel flow with no sodium surface
Secondary heat transfer system (SHTS)	325/529 ℃
Temperature at IHX inlet/outlet	3700 t/h
Flow rate	0.8/0.1 MPa
Main circulatiion pump	One unit per loop
Auxiliary cooling system	By-pass of the secondary cooling system with one air cooler per loop

(b) Locations of plant evaluated high-temperature creep

Location	D (inner dia.) (mm)	t (thickness) (mm)	D/t	Material
RV cylindrical wall	7100	50	142	SUS304 stainless steel
Reactor outlet piping	788	11	72	SUS304 stainless steel
Reactor inlet piping	591	9.5	62	SUS304 stainless steel
IHX vessel cylindrical wall	2940	30	98	SUS304 stainless steel
IHX heat transfer tube	19.3	1.2	16	SUS304 stainless steel
IHX SHTS-side outlet piping	540	9.5	56	SUS304 stainless steel
EV cylindrical wall	2900	50	58	2.25Cr-1Mo steel
Air-cooler heat transfer tube	45	2.9	16	SUS304 stainless steel
Fuel pin cladding	5.56	0.47	11.8	20% cold-worked modified 316 stainless steel

- **The locations with large value of D(diameter)/t(thickness) were chosen for the present calculation of SCDF.**

2.2 Structural analysis ABAQUS 3-d analysis to IHX bottom head - Buckling critical stress and fracture critical stress -

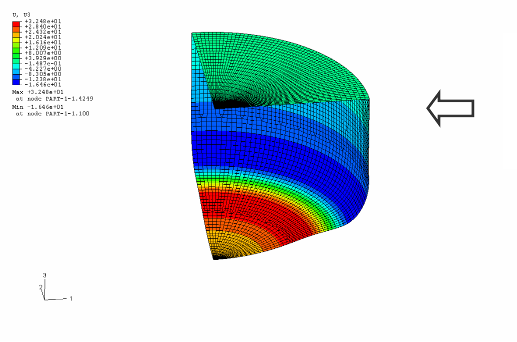

⇦ **The buckling of IHX bottom head became marked at the end of calculation: Temperature: 838.7℃; Pressure: 0.89MPa)**

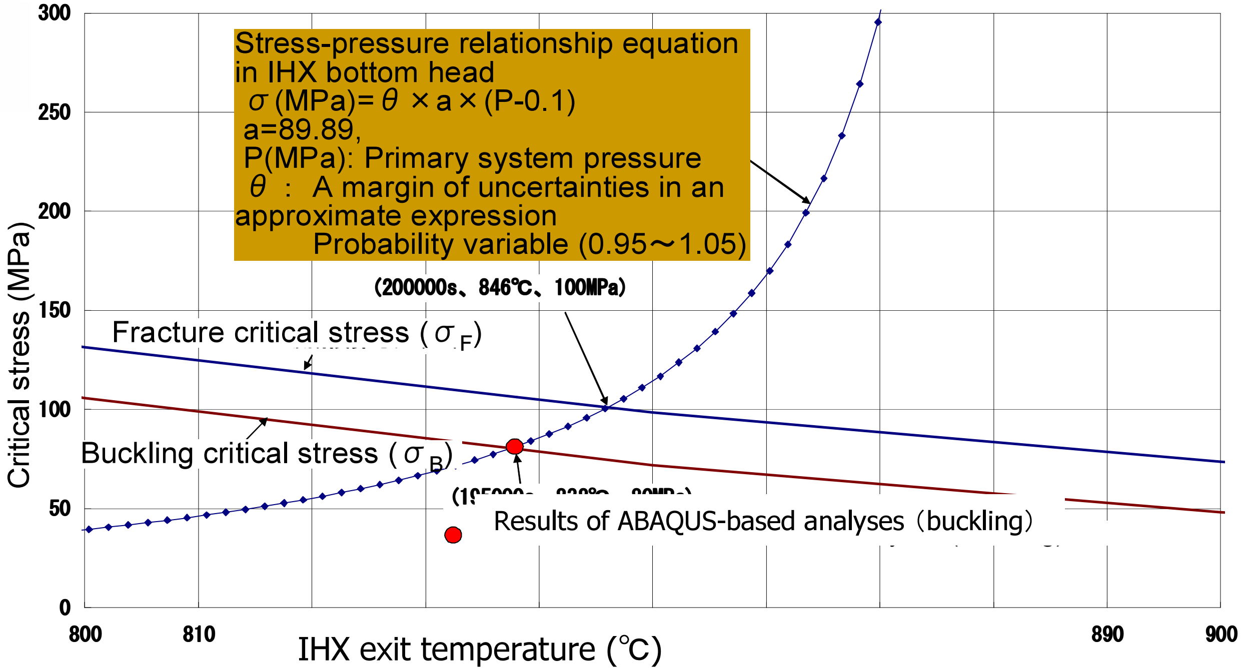

The obtained stress-pressure relation curve encountered with the buckling critical stress line and the fractional critical stress line at one point, respectively. The IHX bottom head is expected to fail at the condition between the two points.

The results of FINAS 2-d analysis to IHX bellows
- Yield stress and tensile stress -

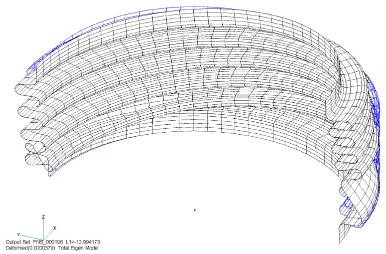

⇦ **Deformed IHX bellows (Temperature: 750℃; Pressure: 0.388 MPa) (The results of the FINAS 3-d calculation**

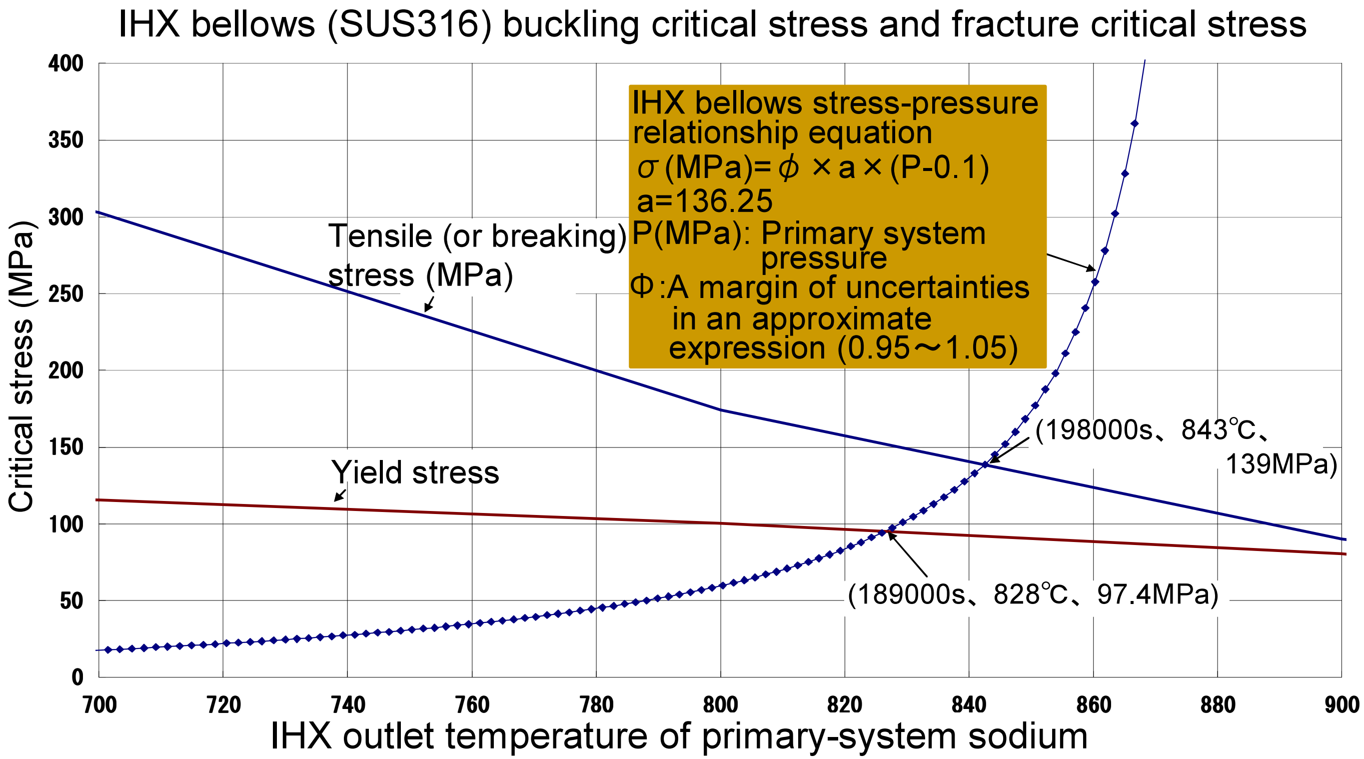

The obtained stress-pressure relation curve encountered with the yield stress line and the tensile stress line at one point, respectively. The IHX bellows is expected to fail at the condition between the two points.

3. Discussion

Pressure range for failure of PHTS components

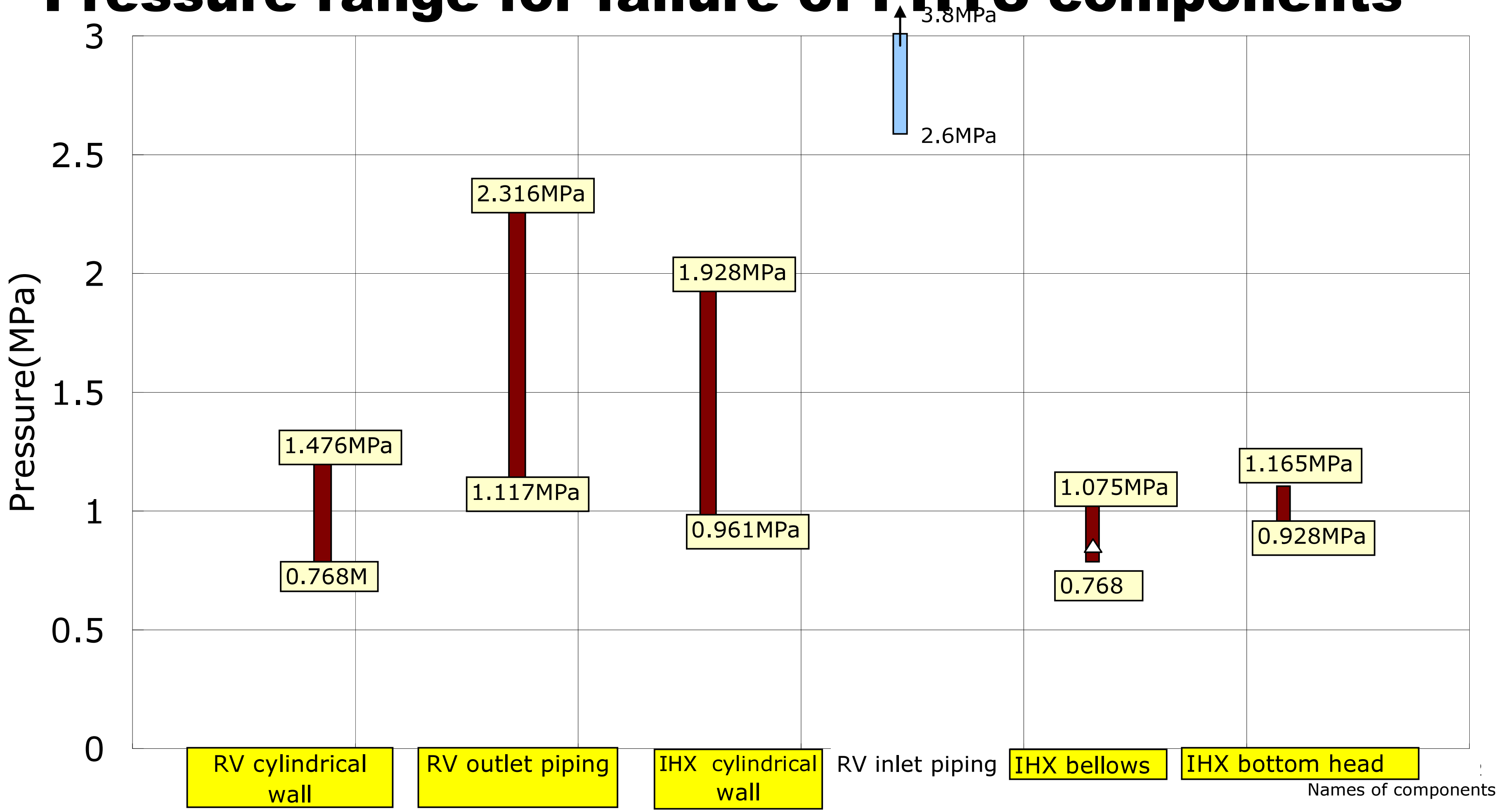

Five locations (RV cylindrical wall, RV outlet piping, IHX cylindrical wall, IHX bellows and IHX bottom head) fail at the pressure between 0.77 to 2.3 MPa) .

Time range for failure of PHTS components

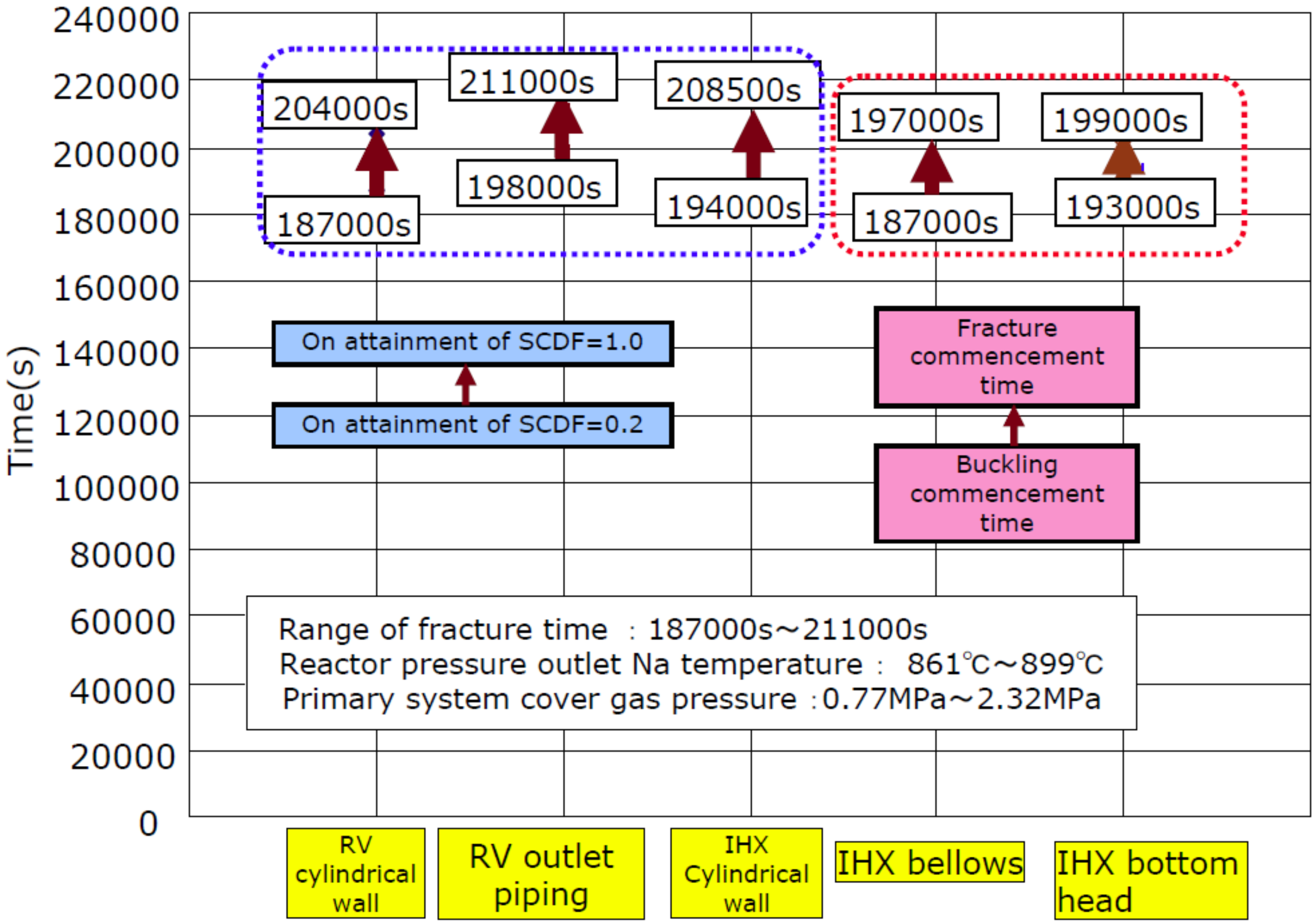

The five locations fail at a narrow time period (between 52hr to 59hr) .

Thus, it will be hard to say the failure order in these locations.

In PSA, it will be reasonable to assign the equal probability of first failure to these locations, that is 0.2.

4. Conclusion

(i) A model to analyze the high temperature creep progression by introducing the calculation function of SCDF was added to the LMFBR plant thermal-hydraulics code, NALAP-II.

（ii）The model was applied to the PLOHS event of the typical proto-type LMFBR. The results indicated that the evaporator made of 2.1/4Cr-1Mo steel in SHTS firstly failed when the system temperature exceeded 800 ℃. The main plant components and piping made of SUS 304 stainless steel failed when the system temperature exceeded 870 ℃.

(iii) In addition, detailed structural analyses were performed by using ABAQUS and FINAS codes and the temperature and pressure histories to the locations where the buckling and the tensile stresses are the causes of failure.

(iv) Comparing the failure time information of each location, it was concluded that the probability of CVBP was 0.2 to the plant.

Appendix –additional information

These numbers were assigned from present study

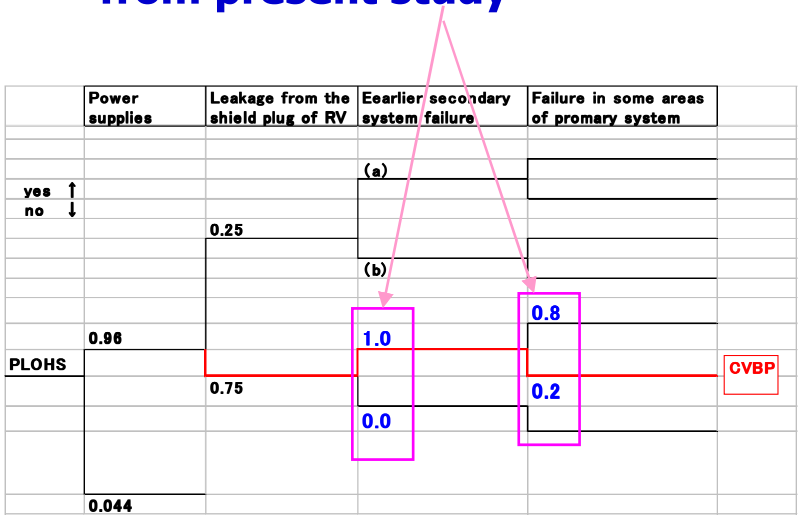

(a) Evaluated provability of the branching points

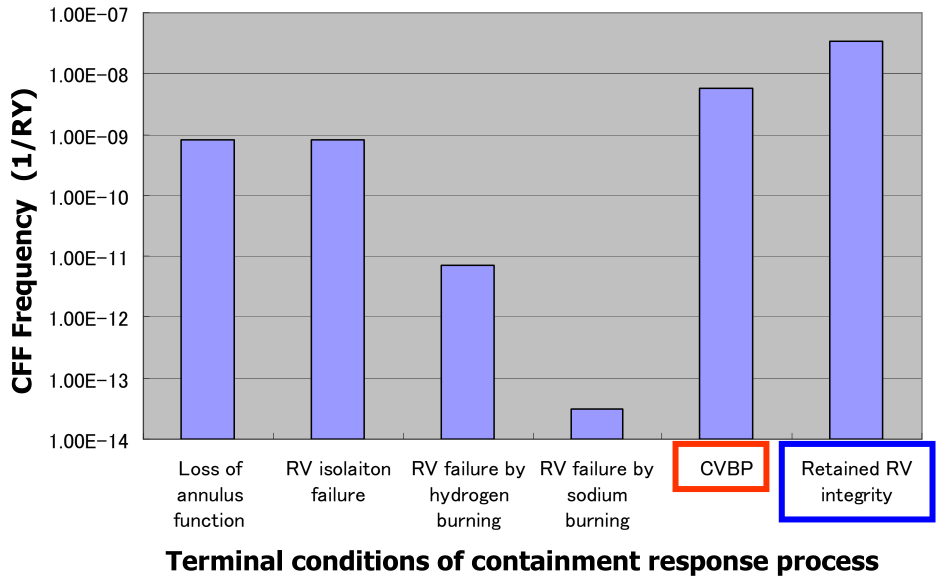

(b) Results of trial evaluation of CFF to each level-2 scenario

Present trial evaluation shows that the frequency of CVBP is one order smaller than that of retained RV integrity scenario. However, the frequency is more than one order larger than that of other scenarios.

Flow network of the NALAP-II code for RV and PHTS

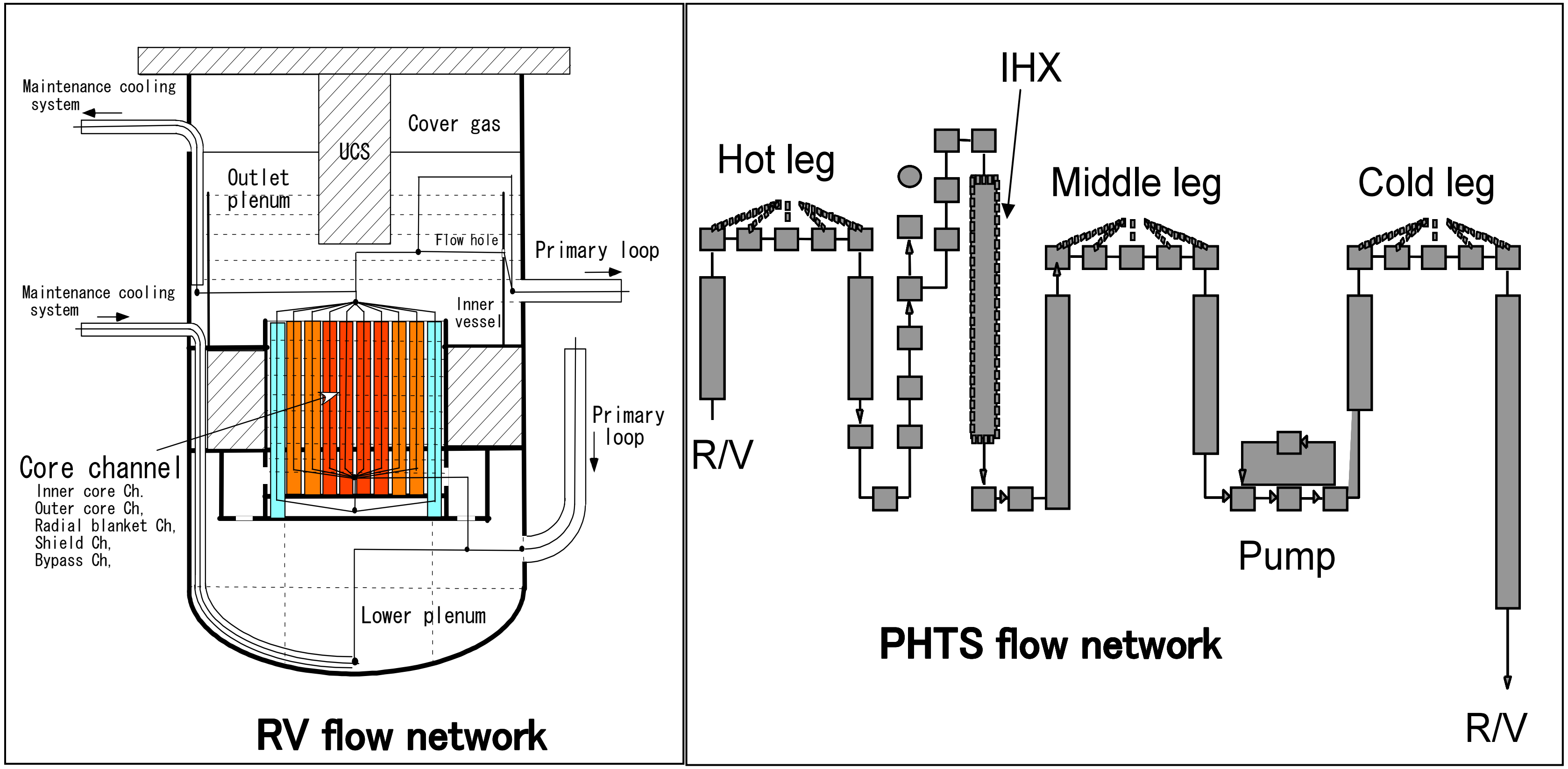

Fig.5 Flow network of the NALAP-II code for RV and PHTS

IHX inlet and outlet temperatures, and PHTS flow rate

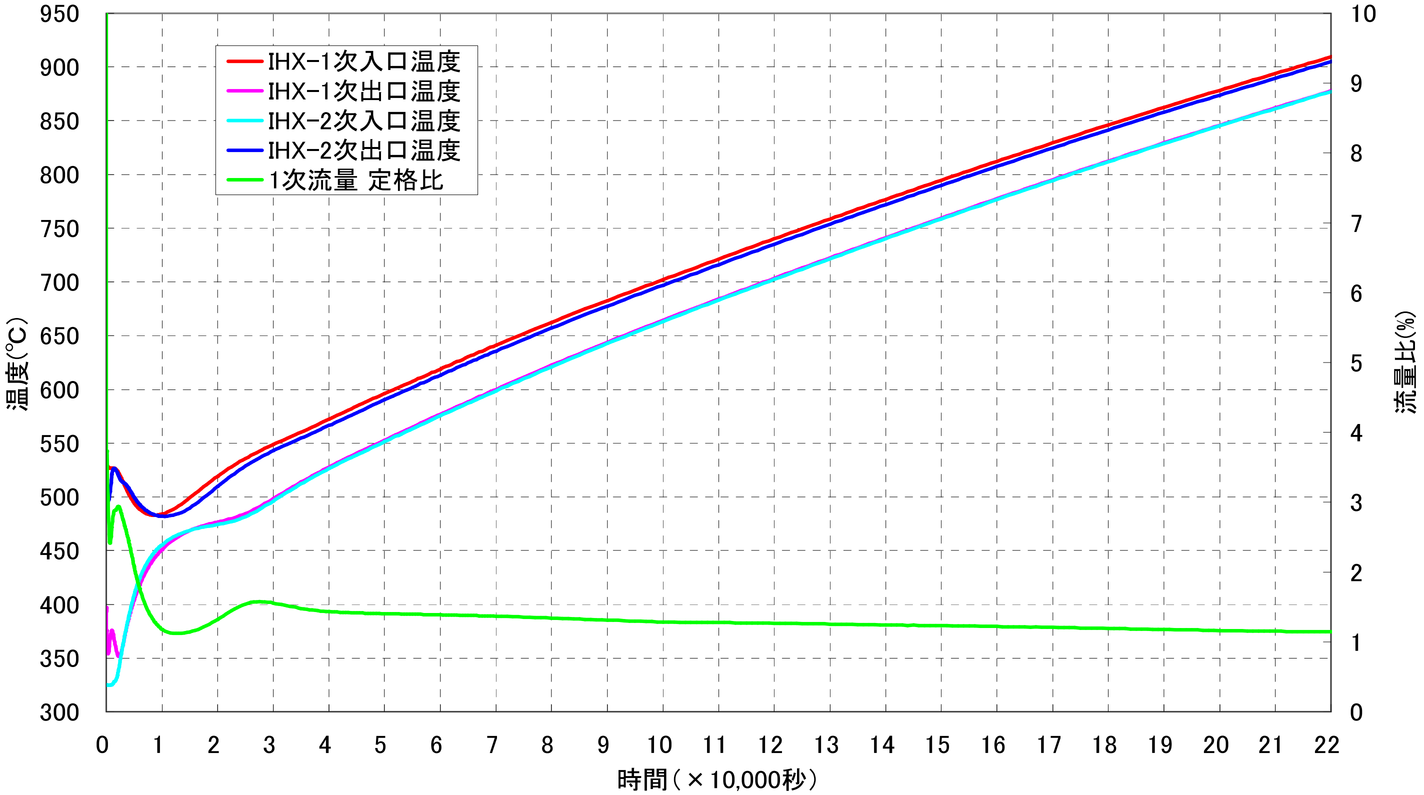

Temperature and the Mises stress behavior of IHX bellows (Stress with the maximal element of equivalent creep strain: the center of plate pressure)

- (The results of the FINAS-based two-dimensional elasto-plastic large=scale deformation and creep analysis)

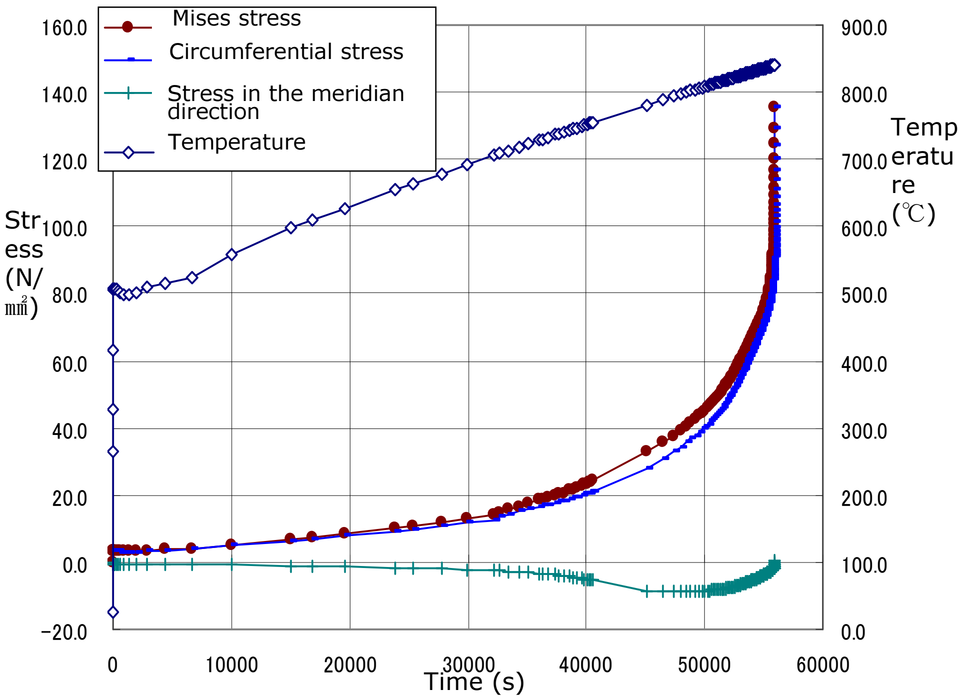

Temperature and the Mises stress behavior of IHX bellows (Stress with the maximal element of equivalent creep strain: the center of plate pressure) (The results of the FINAS-based two-dimensional elasto-plastic large=scale deformation and creep analysis)

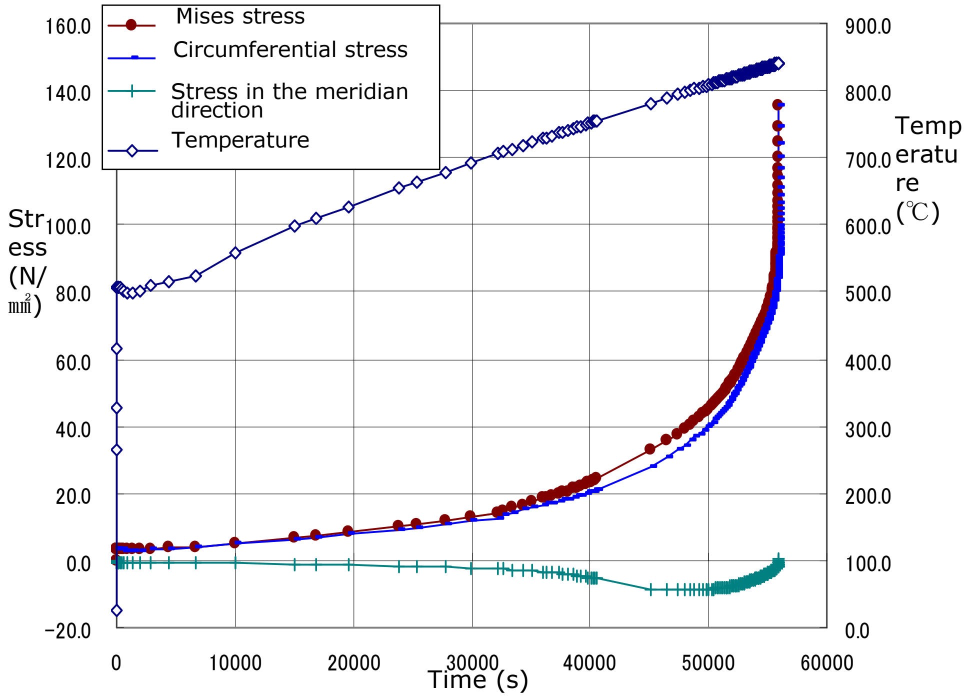

Comparison of initiating events frequency between JAEA and JNES

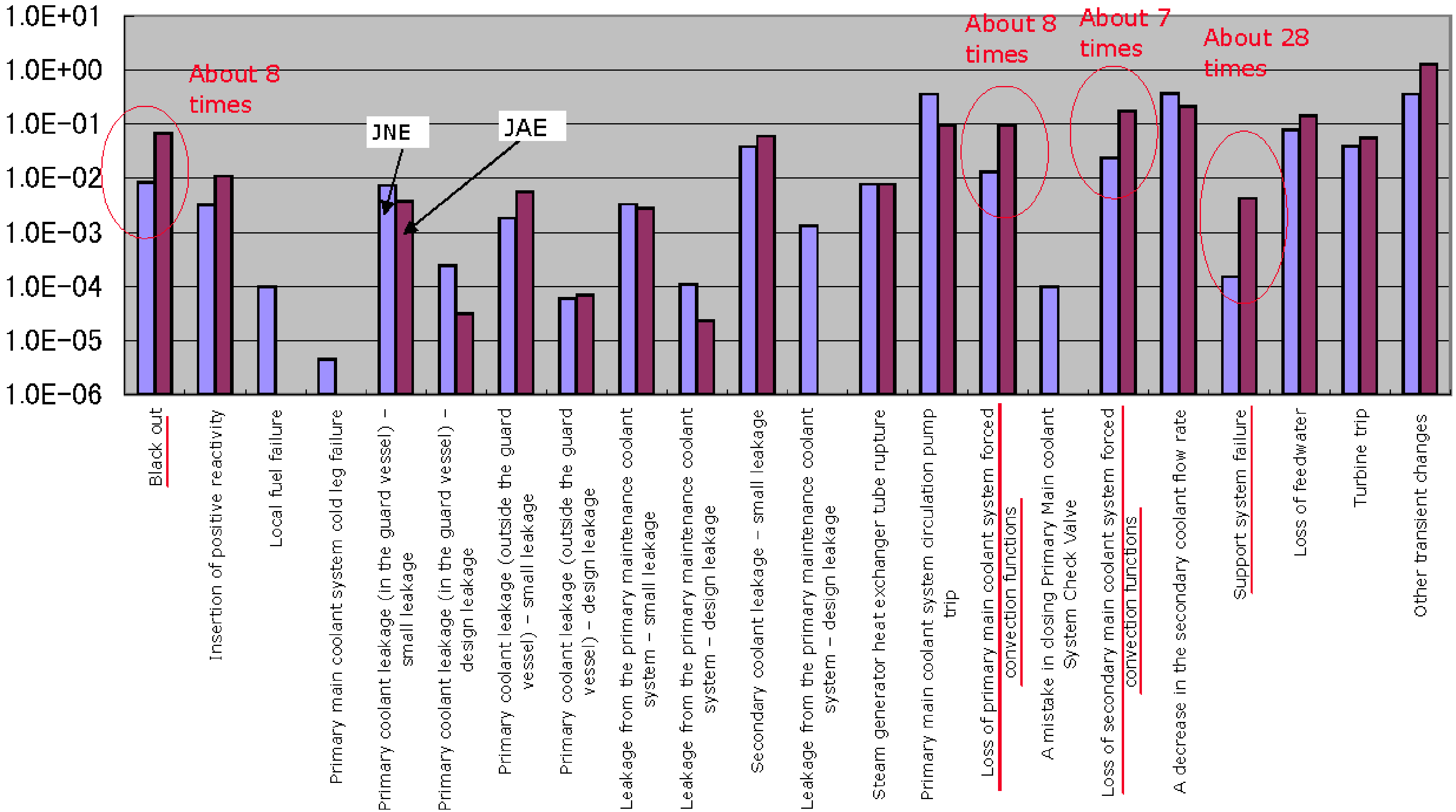

4. Results of PSA

4.1 Effects of AM measures to keep the RV coolant level

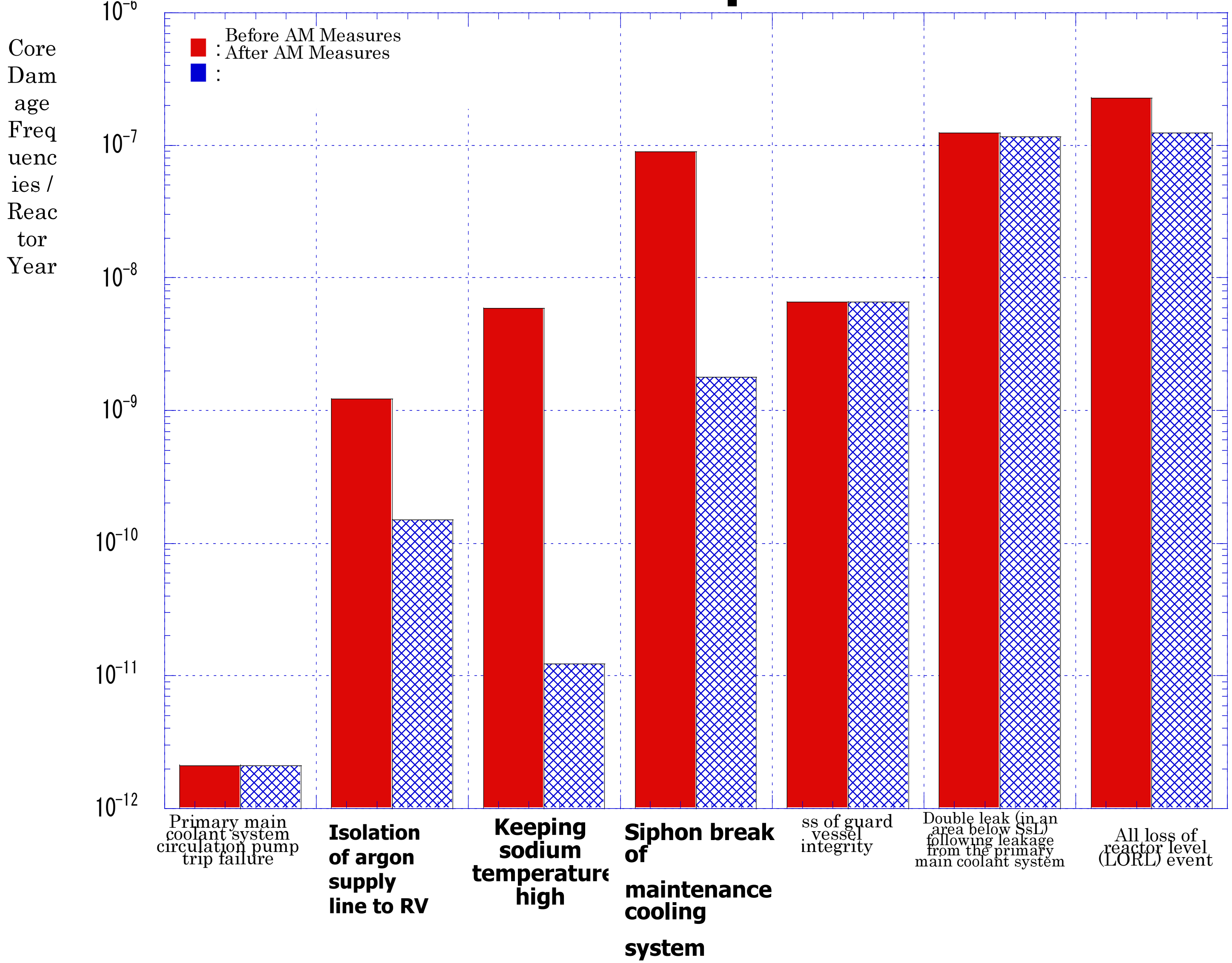

4.2 Effects of initiating events frequency

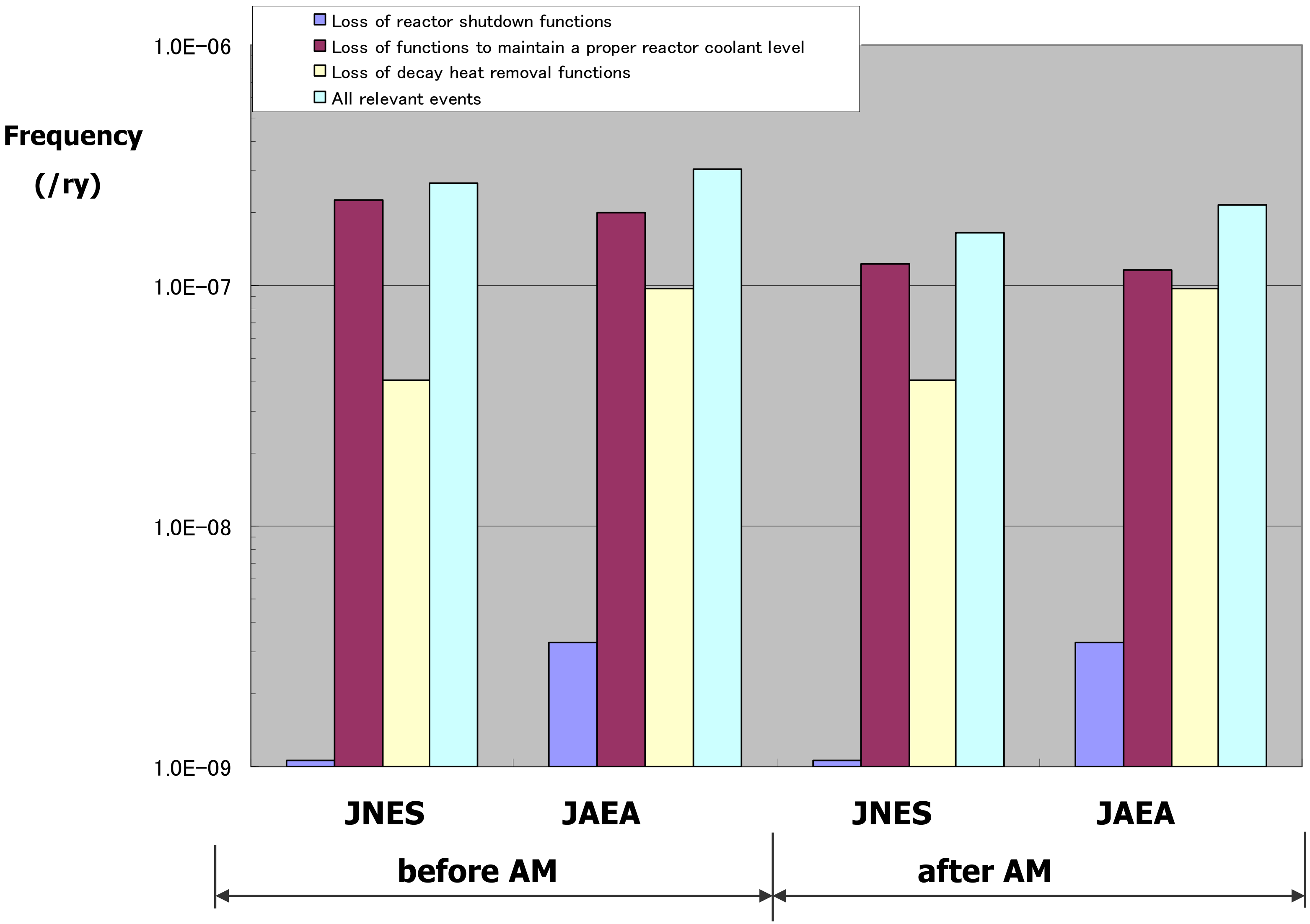

4.3 Effects of choosing common cause failure

(In the PSA of JAEA, common cause failure is considered between the main reactor shutdown system and the backup reactor shutdown system)

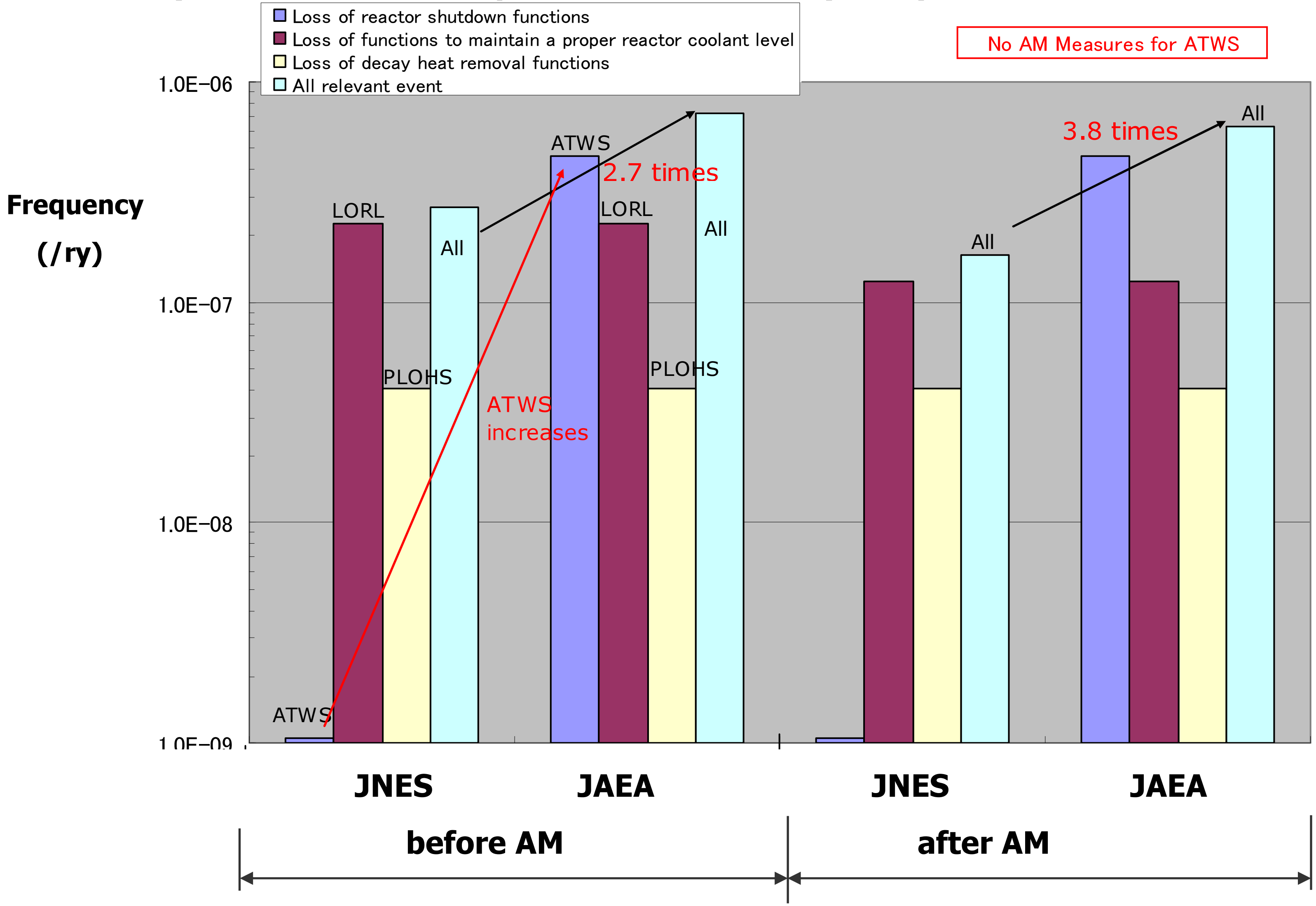

4.4 Contribution of initiating events to CDF (b) after AM （by JNES）

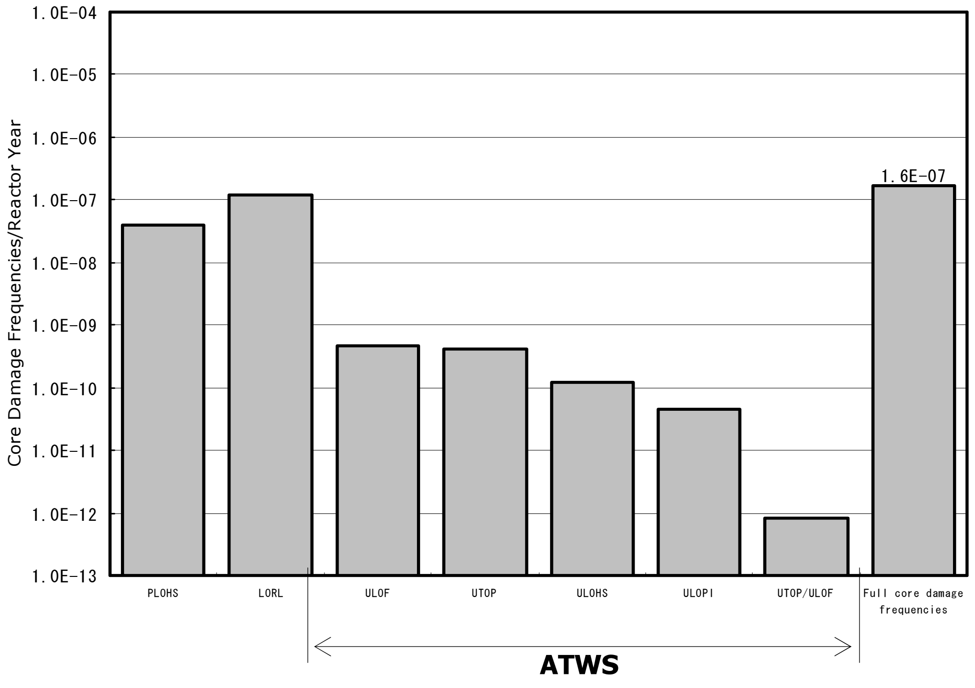

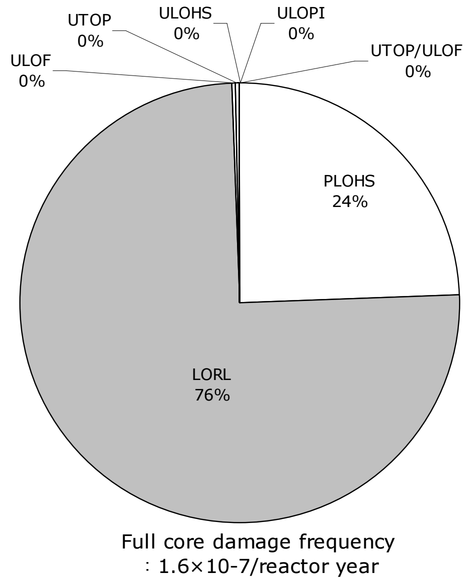

4.5 Comparison of estimated CDF between JNES and JAEA